Workshop on Visualisation in Environmental Sciences (EnvirVis) (2021)
S. Dutta and K. Feige and K. Rink and D. Zeckzer (Editors)

A Virtual Geographic Environment for the Exploration of Hydro-Meteorological Extremes

K. Rink[1], Ö. O. Şen[1], M. Hannemann[1], U. Ködel[2], E. Nixdorf[1], U. Weber[3], U. Werban[2], M. Schrön[2], T. Kalbacher[1], O. Kolditz[1,4]

[1]Department of Environmental Informatics, Helmholtz Centre for Environmental Research, Leipzig, Germany
[2]Department of Monitoring and Exploration Technologies, Helmholtz Centre for Environmental Research, Leipzig, Germany
[3]Department of Computational Hydrosystems, Helmholtz Centre for Environmental Research, Leipzig, Germany
[4]Chair of Applied Environmental System Analysis, TU Dresden, Germany

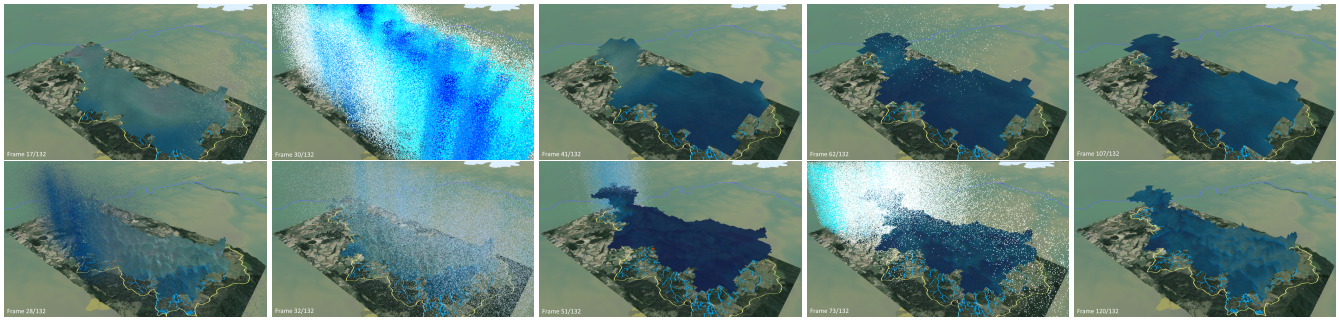

Figure 1: *Synchronous animation of transient phenomena: Concurrent visualisation of selected frames of observed precipitation data and simulated soil moisture fluctuation for two rain events between 10 and 14 June 2019. The upper row shows selected time steps of a simulation result for a model with a spatial resolution of* 1000 *m, the lower row shows frames from a model with* 200 *m resolution, offset by a few frames from the upper row. Starting at reasonably dry conditions, a heavy rain event at 10 June results in a delayed increase of soil moisture in the region. A second event in the north of the catchment on 12 June (left-hand side of the images) keeps the soil moisture content high, while it starts dropping again towards the south (right-hand side).*

Abstract

We propose a Virtual Geographic Environment for the exploration of hydro-meteorological events. Focussing on the catchment of the Müglitz River in south-eastern Germany, a large collection of observation data acquired via a wide range of measurement devices has been integrated in a geographical reference frame for the region. Results of area-wide numerical simulations for both groundwater and soil moisture have been added to the scene and allow for the exploration of the delayed consequences of transient phenomena such as heavy rainfall events and their impact on the catchment scale. Implemented in a framework based on Unity, this study focusses on the concurrent visualisation and synchronised animation of multiple area wide datasets from different environmental compartments. The resulting application allows to explore the region of interest during specific hydrological events for an assessment of the interrelation of processes. As such, it offers the opportunity for knowledge transfer between researchers of different domains as well as for outreach to an interested public.

Categories and Subject Descriptors (according to ACM CCS): I.3.3 [Computer Graphics]: Three-Dimensional Graphics and Realism—Virtual reality

1. Motivation

With the effects of climate change becoming more noticeable every year, the understanding of both, long-term trends and impacts of short-term extreme weather events, becomes more and more important. There is substantial evidence that climate change will be associated with an increase in frequency, intensity or a shift in timing of weather extremes such as heavy rains and droughts, elevated flooding and extended low water periods, all with as yet un-

DOI: 10.2312/envirvis.20211084

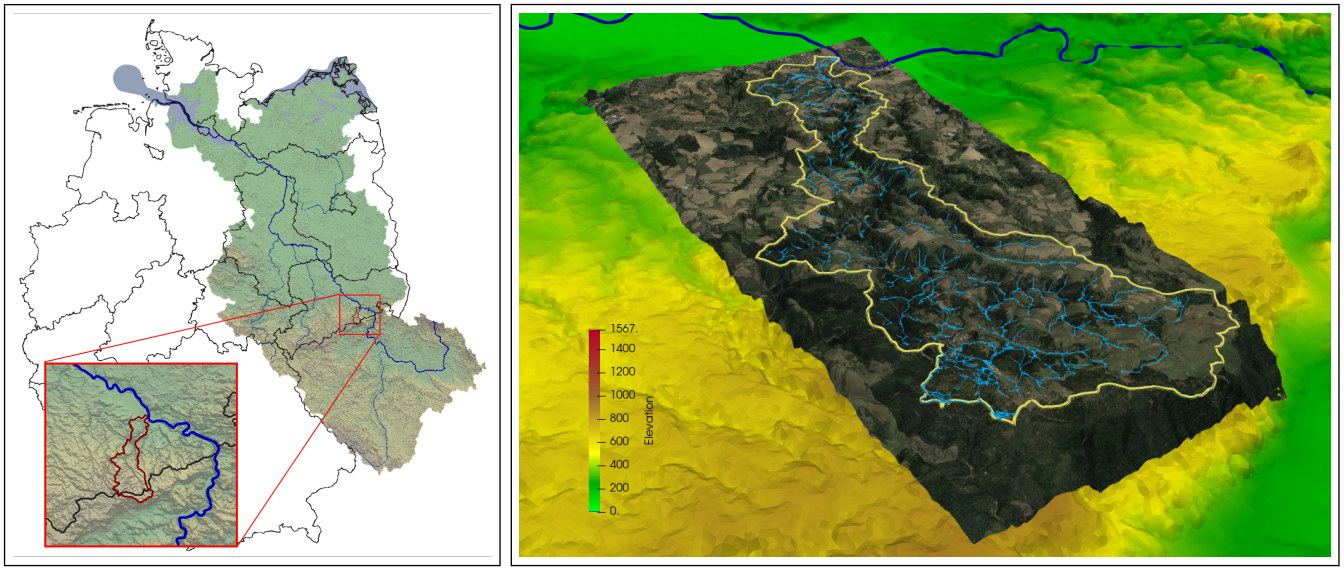

Figure 2: ***Left:*** *Location of the Müglitz catchment within the catchment of the Elbe River and in relation to the German states.* ***Right:*** *3D surface of the catchment area serving as a reference frame for hydrological datasets. The boundary of the catchment is marked in yellow, streams are depicted in blue. Near the upper image boundary, the Müglitz River can be seen joining the Elbe River (represented by the thick blue line) in Heidenau, just southeast of the city of Dresden.*

foreseeable environmental and socioeconomic consequences. Such meteorological and hydrological extremes are restricted in time and they are spatially distinct, but their ultimate impact may be significant for much larger regions (e.g. the downstream catchment areas flooded from run-off generation in upstream headwaters) and with delayed effects (e.g. algal blooms in coastal zones triggered by legacy nutrient pulses from inland sources). The new MOSES (Modular Observation Solutions for Earth Systems) observing system is being developed to monitor the evolution of such weather extremes and their impacts on the affected regions. It comprises mobile and modular sensor systems which record energy, water, greenhouse gases and nutrient cycles in the atmosphere, on the land surface and in coastal regions – but especially the interactions between environmental compartments and the affected ecosystems. The underlying observation concept systematically combines MOSES' event-oriented measurements with stationary integrative monitoring programmes and observatories which are mostly designed for long-term, large-scale environmental observation. The catchment of the Elbe River, the fourth largest river in Europe based on the size of its catchment, is one of MOSES' target areas because it has been frequently affected by extreme low flows and severe floods: In 2018 and 2019 historically low river flows and high water temperatures caused fish mortality and algal blooms in the down-stream region. This decline in water quality was accompanied by increased sedimentation of the Tide-Elbe up to the port of Hamburg. On the other hand, the floods of 2002 and 2013 lead to widespread flood defence failures and disastrous damages. One of the most affected regions was the Müglitz Valley in the Saxonian Ore Mountains where the highest daily rainfall ever measured in Germany caused a catastrophic flash flood in 2002. For the entire region, a better understanding of hydro-meteorological extremes and their impact is crucial to minimize future risks and damages.

To foster communication between the researchers conducting observations within the MOSES initiative and as a means to reach out to the interested public, a virtual geographic environment has been created for the Müglitz Catchment. A large collection of free datasets and observation data acquired via the MOSES measurement campaigns has been integrated into the prototype of a VR application, as a means to assess how the various datasets correlate and interact with each other and to have a unified context of data acquired via observation and numeric modelling.

Section 2 gives a short overview of the use of Virtual Geographic Environments for the visualisation and exploration of environmental data collections. Details on the datasets used for this particular study in the scope of MOSES are presented in Section 3. The resulting application is discussed in Section 4. Conclusions as well as an outlook are given in Section 5.

2. Virtual Geographic Environments

The representation of all available data for an environmental study in a unified geographical context has become more and more important in recent years [LCL*13, LYZ*15, GFW17, RNZ*20]. The task is not trivial, as datasets are acquired by different means can have very different properties. Typical examples of datasets for an environmental study usually include satellite data (e.g. aerial imagery, digital elevation models, hyperspectral data, etc.), vector data (boundaries, rivers, streets, boreholes, etc.), and point data (observation sites, wells, etc.). Additional information may be attached to any of those datasets, such as measured parameters at an observation site (i.e. time series data) or concentration of chemical ele-

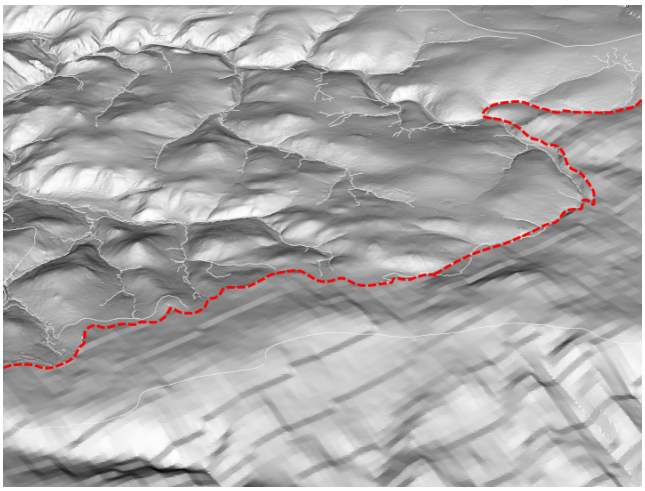

Figure 3: *Topological surface based on a high resolution digital elevation model (DEM) for the part of the catchment located in Germany and a coarse DEM for the part located within the Czech Republic. (Red line added for illustration purposes.)*

ments along a river. In addition, datasets often vary in their extent, resolution, or specific properties such as the geographic projection or already applied preprocessing techniques (e.g. raw data vs sliding mean for temperature measurements).

Virtual Geographic Environments (VGEs) are based on Ellis' definition of "virtual environments" [Ell94] and Batty's treatise on "virtual geography" [Bat97]. VGEs facilitate an immersive, interactive experience of geographic or, by extension, environmental data within a synthetic space. Early examples have been proposed as an extension of geographic information systems (GIS) into 3D and virtual reality [Bat08, Yin10]. Lin et al. [LCL*13] extended this approach by including simulation results of numerical models as well as adding collaborative components to the immersive 3D visualisation of heterogeneous data. A number of very advanced 3D frameworks exist for the visualisation of meteorological data [KHS*18, KvdN18], displaying complex processes in the atmosphere and comparing observed and simulated data. Due to the large extent of selected regions, the surface of the Earth is usually displayed as a 2D plane (often a map), while subsurfaces processes are ignored completely. While this makes sense in the scope of these applications, we are aiming for a multi-compartment visualisation of meteorological phenomena as well as processes on and below the surface.

The VGE framework presented here is an extension of the framework previously employed for hydrological studies on Chinese lake catchments [RCB*18, RNZ*20]. It is based on Unity [Uni20] and offers a range of methods to import, visualise, and interact with environmental data. Datasets are preprocessed using the OpenGeoSys Data Explorer [RBK14] or ParaView [AGL05], both of which employ VTK data structures and algorithms [SML06] to represent 3D objects.

3. Case Study: Catchment of Müglitz River

The focus of this particular study and one of the intensive test sites of the MOSES initiative is the catchment of the Müglitz River, covering about $209\,km^2$ in the Ore Mountains between Germany and the Czech Republic. The river flows from South to North, has a length of $50\,km$ and is a tributary to the Elbe River, the fourth largest river in Central Europe based on the size of its catchment (see Fig. 2a). The narrow mountainous catchment consists of steep valleys and agriculturally used plateaus covered by shallow soils. Low pressure systems originating from the Mediterranean Sea which move northward can result in intense orographic induced rainfall in the catchment. In interaction with the geomorphological characteristics, these intense rainfall events can initiate severe flash floods. For example, in August 2002, with more than $300\,mm$ precipitation within 24 hours, the highest daily rainfall ever measured in Germany until today, resulted in massive destruction of the infrastructures along the entire valley. Hence, an enhanced understanding of the factors driving the hydrological response of the Müglitz River Basin on intense precipitation events as well as the consequences for the Elbe River Basin are of particular interest. Subsequently a large collection of environmental data has been measured and collected by MOSES in the catchment over the past years.

As a frame of reference, a model of the geography of the region has been set up. As a first step, a (georeferenced) rectangle containing the catchment of the Müglitz river has been defined and tesselated. The elevation for the nodes of the resulting grid has been mapped based on DGM2 data for the German part of the catchment and interpolated from SRTM data for the Czech part. DGM2 is a digital elevation model at a resolution $2\,m$, provided free of charge by the state of Saxony [Sta15]. SRTM data, acquired via the Shuttle Radar Topography Mission, is a dataset of worldwide digital elevation provided by NASA with a resolution of one arc second (ca. $30\,m$) [Uni18]. The resulting 3D surface consists of 3.2 mio triangles with an average edge length of $25\,m$ (see Fig. 3). A reasonably fine triangulation is important here, as this is a mountainous region where the valleys created by streams cause steep gradients on the surface. A high resolution aerial image with a resolution of 6000×12000 pixels [Bun21] has been applied as a texture on the 3D surface. For orientation, both the boundary of the catchment of the Müglitz river as well as a dataset containing all streams within the catchment have been mapped onto the 3D surface (see Fig. 2b).

Based on this georeferenced surface, both hydrological observation data as well as results of numerical simulations have been added to the scene. In particular, this includes RADOLAN rainfall data provided by the German Weather Service [Deu19] at a spatial resolution of $1000\,m$ and a temporal resolution of one hour. An integral annual average estimation of groundwater recharge is provided for each of the 172 main sub-catchments of the Müglitz River Basin by water balance modelling [SHB*14].

Initiated by MOSES, two extensive measurement campaigns were launched within the catchment in 2019 and 2020, including stationary observation sites measuring parameters such as soil moisture, temperature, or discharge (see Fig. 4b). In addition, multiple times per year measurement devices mounted on mobile equipment were used to get measurements over a larger area within the catchment. This includes Cosmic Ray Neutron Sens-

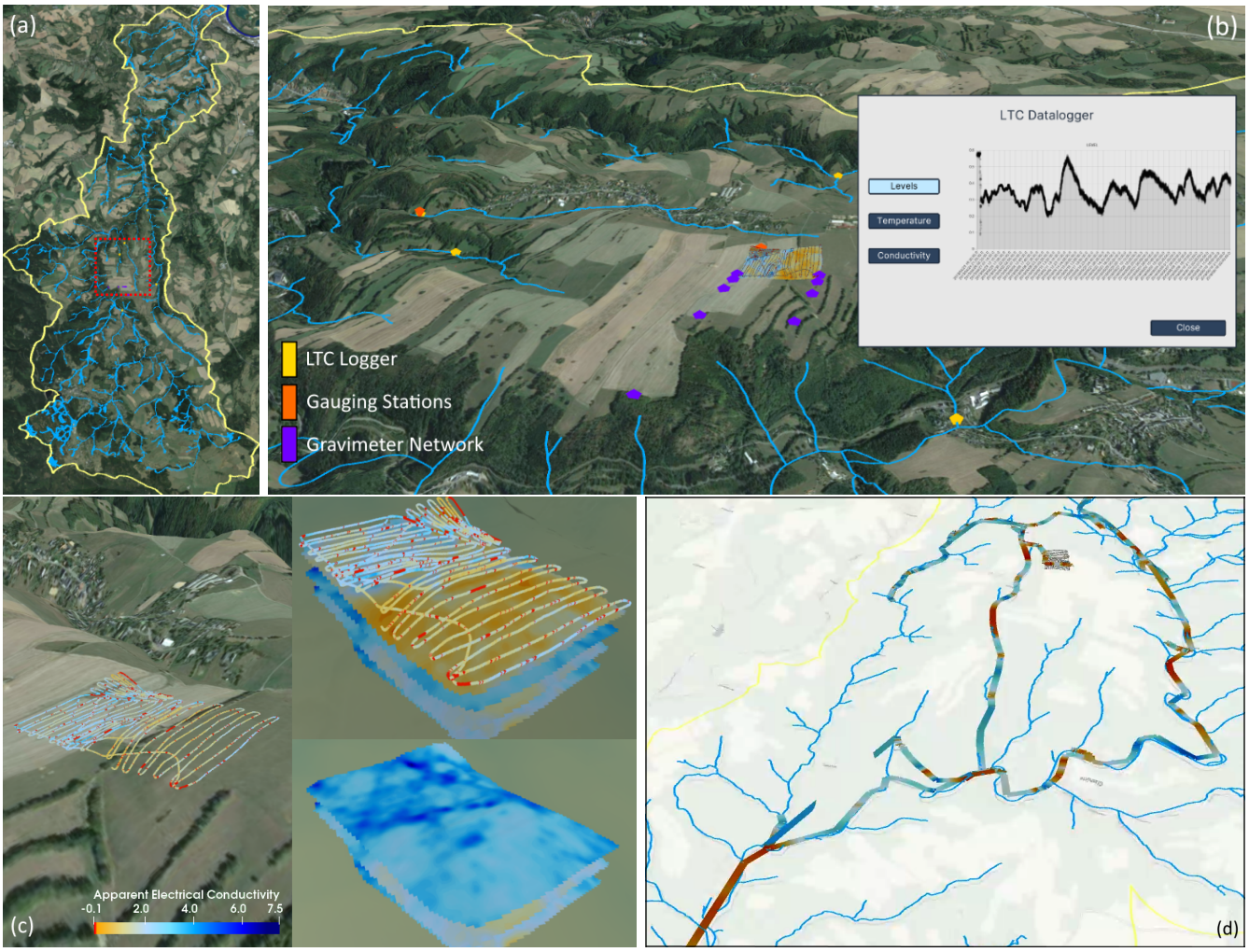

Figure 4: *Examples for observation data acquired within the Müglitz Catchment and integrated into the VGE:* ***(a)*** *overview of the catchment, highlighting the intensive test site located in the centre;* ***(b)*** *locations of data loggers, specifically gauging stations displayed in orange, LTC data loggers (measuring water levels, temperature, and conductivity) displayed in yellow, and a gravimeter network displayed in violet. Time series data can be linked to each object, so that 2D plots will be generated upon clicking on any of the observation sites;* ***(c)*** *visualisation of electromagnetic induction data: Shown are both the original tracks of the vehicle as well as interpolated values for the complete field. Measurements a various depths can be interactively cycled via the user menu;* ***(d)*** *illustration of the CRNS data: Generated line strips display the derived soil moisture at each location, mapped onto what OpenStreetMap calls a "positron map" for better visibility.*

ing (CRNS), electromagnetic induction, and a geophysical gamma-ray spectrometer for field measurements. CRNS is a measurement technology based on the generation of fast neutrons by cosmic rays, their moderations by collisions with hydrogen and backscattering into the atmosphere. CRNS utilises naturally occurring cosmic ray neutrons as a proxy for soil water content over a large lateral radius of approximately $260\,m$. The sample depth is integrated over the top several decimetres and varies from 0.1 to $0.6\,m$, depending on the existing soil water content [Des17]. A data logger records the raw neutron counting rate and various meteorological parameters such as barometric pressure, temperature, and relative humidity. Several corrections of these observations are required based on barometric pressure, solar activity, and absolute humidity. In addition to soil moisture, specific characteristics of the environment are sources of hydrogen. Therefore, further post-processing might be required, for instance based on vegetation or road effects [BBH*15, SRK*18]. Being deployable on cars, the mobile application of CRNS is a promising approach to measure field soil moisture content noninvasively by surveying large regions [SRK*18]. During the 2019/2020 measurement campaigns, CRNS measurements were acquired on 31 separate days, each resulting a dataset of ranging from a few hundred to several thousand spatially and temporally referenced data points representing the route of the rover over the course of the day as well as neutron count and derived soil moisture at each location and time (see Fig. 4d).

For electromagnetic induction measurements (EMI), two sensors were used to measure the apparent electric conductivity (ECa in mSm^{-1}) to characterize the subsurface. ECa is closely related to numerous soil properties, such as texture, bulk density, soil organic carbon, and soil moisture [CSC16, MWZ*17]. Both devices have one transmitter and three receiver coils with different intercoil spacings. A primary magnetic field is generated by an alternating current flowing through a transmitter coil, which causes eddy currents in the conductive underground through induction. Together with the primary magnetic field, the resulting secondary magnetic fields are registered by a receiver coil. The penetration depth of the magnetic field increases with larger intercoil spacing and can be further controlled by the orientation of the dipoles and the applied frequency [RWA*20], allowing for simultaneous multi-depth exploration of ECa. The measurement devices were mounted on a sledge and towed by a four-wheel vehicle at a speed of less than $10 km h^{-1}$ in multiple parallel and a few crossed transects across a field selected as an intensive test site. As a result, measurements have been obtained at six different effective penetration depths in intervals ranging from $0.9 m$ to $6.7 m$. The resulting datasets consists of ca. 9500 data points per layer per day. A subsequent interpolation of these measured tracks resulted in four layers showing apparent electric conductivity at different depth on a field scale (see Fig. 4c).

The gamma-ray spectrometer determines the concentration of Kalium (K), Uranium (U) and Thorium (Th) and the natural gamma dose rate in $Gy h^{-1}$. According to Cook et al. [CCGG96], 90% of above-ground measured gamma radiation is emitted in the top $30-50 cm$ of soil. The concentration of detected radioactive nuclides can be influenced by mineralogy, soil texture and is linked to pH, soil organic carbon content, and soil water content [DW13]. A gamma-ray spectrometer with a $4l$ sodium-iodide ($NaI(Tl)$)-crystal and automatic peak-stabilization was mounted on a sledge, similar to the EMI sensors. On the same field, measurements for ^{40}K, ^{238}U, and ^{232}Th were obtained in counts per second. Subsequently, the concentration was calculated corresponding to the decay rate at specific energy levels.

In addition to the integration of observation data, two numerical models for the region have been prepared, simulating processes relevant for the water cycle: Based on the geography, subsurface, and precipitation data, a steady-state groundwater model has been set up using the FEM-based OpenGeoSys simulation software [KBB*12]. The two-dimensional model provides a reference for the distribution of groundwater levels and subsurface flow dynamics in this basin. In addition, a transient hydrologic model for the Müglitz river basin was developed using the software mHM to simulate soil moisture and river discharge with a temporal resolution of one day. mHM is a spatially distributed hydrological model with raster cells as primary hydrologic units. It uses multiscale parameter regionalisation, allowing to choose different grid cell resolutions for meteorological and morphological input datasets [SKA10, KSA13]. The hydrologic model was calibrated on a gauging station within the basin for a period of 13 years between 2007 and 2020, including a spin-up time of two years. This period includes various hydrologic conditions, including the previously mentioned extreme flood event in 2013 and the drought in 2019. The model was forced with meteorological data (e.g., precipitation) on a $1000 m$ grid. Morphologic input data, such as a map of locally distributed soil types derived from the BK50 dataset [Sae20] was used with a spatial resolution of $100 m$. The simulation of hydrologic states and fluxes was carried out on a $1000 m$ grid; and additionally on a $200 m$ grid to enable a more detailed blending with the other datasets used for our visualisation. At both resolutions, the model can be employed to get an estimate for catchment-wide soil moisture at different depths instead of in selected locations only.

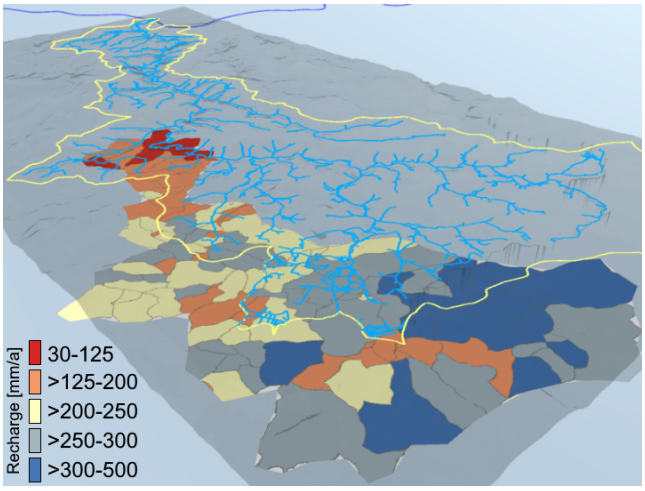

Figure 5: *Steady-state groundwater model of the Müglitz Catchment. The triangulated surface is warped based on the simulated groundwater head and located at an offset below the topological surface. A map of groundwater recharge zones [SHB*14] can be optionally mapped onto the surface, additionally identifying zones based on their annual groundwater recharge.*

4. Virtual Environment

All datasets introduced in section 3 have been projected into the spatial reference system EPSG:32633 (WGS84/UTM Zone 33 North), the appropriate UTM zone for eastern Germany and the Czech Republic, and thus for the Müglitz catchment. As a result, no manual adjustments are required for the correct positioning of datasets in the XY-plane. A grid representing the topological surface of the region has been built based on the DGM2 data and a high resolution aerial image has been applied as a texture to serve as a reference frame for the visualisation of the observation and simulation data collection in the scope of the project. 2D datasets, such as the streams within the catchment as well as the cosmic ray- and electromagnetic induction data, have been mapped onto the topological surface using the approach proposed in [RBK14] (see Fig. 4).

Corresponding to the MOSES initiative, this study is meant to demonstrate the interactions of short-term events and long-term trends. As an example, we focus on two rain events between 10 and 14 June 2019 and the subsequent changes to soil moisture (see Fig. 1). While the representation of both, the topological surface and vector data such as boundaries or streams, is fairly straightforward, finding suitable metaphors for the soil moisture simulation results and the precipitation data presents a challenge. Both data-

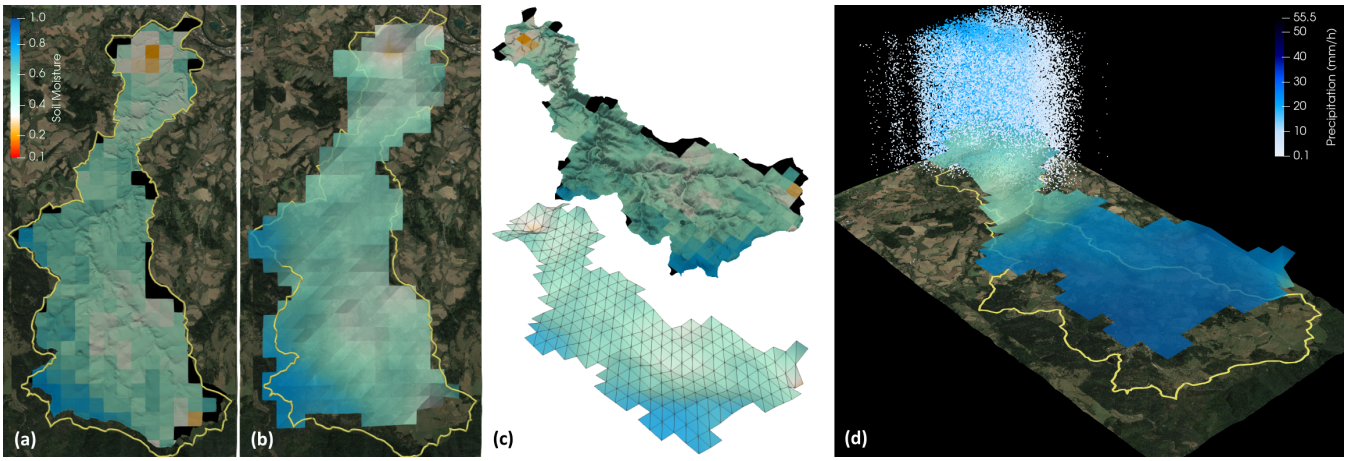

Figure 6: *Visualisation of the topsoil layer of volumetric soil moisture simulated via the hydrological mHM model.* ***(a)*** *Mapping simulation results directly onto the 3d surface from an early prototype,* ***(b)*** *current representation of simulation results as separate 3d surface,* ***(c)*** *isometric view of both approaches,* ***(d)*** *final representation of concurrent visualisation of surface, simulation results and precipitation data.*

sets are originally stored as time series of raster data. In addition, a concurrent animation for both is required, so the consequences of precipitation for soil moisture become visible with the appropriate delay. The original approach of mapping the simulation results onto the topological surface was quickly rejected (see Fig. 6a). Not only does this representation remove any reference information gained from the aerial imagery, but the large differences in resolution (25 m for the topological surface vs 1000 m for the simulation results) make it difficult to process the displayed information visually. In addition, due to the large differences in spatial resolution, parts of topological surface are not represented in the simulation while at the same time simulated data is missing as it is located outside the catchment. In the current prototype of the application, soil moisture is therefore represented as a separate 3D surface layer located above the topological surface. High soil moisture is represented by both a larger elevation of the mesh nodes as well as by colour (see Fig. 6b). This way, changes in soil moisture values are easily visually processed while keeping the geographical reference frame. The colour transfer function used for the soil moisture simulation, as well as for the CRNS- and EMI-measurements (Figs. 4 and 6) is based on the colour lookup table used for the UFZ drought monitor, an interactive web service provided by our research centre for information on soil moisture for the whole of Germany (https://www.ufz.de/droughtmonitor/). The vertical translation of the layer of simulation results should be not much larger than the maximum elevation of the topological surface. A smaller offset may result in both surfaces intersecting, a larger offset will reduce the visual correlation with the geographical reference frame. Occlusion of one surface by the other can be a problem, but is mitigated by users being able to freely navigate within the scene and the possibility of interactive adjustment of opacity values for all datasets. Increasing the transparency of the simulation results can be arranged either as a preset, as a scripted event or interactively during runtime (while possibly pausing the animation).

For precipitation data, we chose a visual metaphor first introduced in [RNZ*20], where cumulative rainfall per time step (i.e. per hour) is represented as a point cloud. The higher the amount of rain, the larger the amount of points within the geographical region represented within each pixel of the precipitation dataset. Specifically, for each pixel i in every time step t in the precipitation dataset, the number of points n_i^t is calculated as

$$n_i^t = (n_{max} - n_{min}) \left[\frac{p_i^t - p_{min}}{p_{max} - p_{min}} \right]^{\gamma} \quad (1)$$

where p_{min} and p_{max} are the minimum and maximum precipitation over the whole time series (p_{min} will usually be 0) and p_i^t it the precipitation given pixel i at time step t. A variable γ determines the increase of points with increasing precipitation and $(n_{max} - n_{min})$ is a scaling factor based on the the maximum and minimum number of points set for each pixel, respectively (again, n_{min} will usually be 0). While point clouds were regarded a suitable representation for rainfall before, researchers have noted that it was difficult to correctly assess the amount of precipitation. Therefore, this approach was adjusted for this case study by additionally applying a global colour transfer function to the data based on p_i^t, as colours can be visually well categorised, especially given an optionally displayed colour legend. The colour transfer function used ranges from white for little precipitation to dark blue for very large amounts of rain (Fig. 6d). This is basically the same transfer function as used for soil moisture related data, minus the red/yellow interval reserved for dangerously low values of soil moisture. Another extension of our framework fades transient datasets between subsequent time steps, allowing for a smoother animation of data that would otherwise result in sudden abrupt changes. We have applied this feature to the animation of precipitation data point clouds (available at 1 hour intervals), soil moisture simulation results (available at 24 hour intervals) – both shown in Fig. 1 – as well as the animation of the various layers of the EMI measure-

ments (Fig. 4c). The case study also includes the results of the groundwater simulation, rendered as a warped surface representing the groundwater head. Again, the visual metaphor can be additionally supported by a colour transfer function. A map of groundwater recharge zones [SHB*14] can be optionally mapped onto the surface to provide additional information (Fig. 5). Although changes in the groundwater table happen considerably slower than for other processes illustrated in this application, a simulation result was included here as to account as a reference for this part of the water cycle.

Another addition to our framework first introduced in this case study aims at keeping the amount of input data as small as possible, both in terms of required storage space and time required to load data. Datasets consisting of large amounts of point data (such as precipitation, CRNS-, and EMI measurements) are only processed at runtime using distinct geometry shader batches on the GPU. Geometry shaders are being employed for transform feedback, to display an arbitrary shape at each vertex of the point data set by creating intermediary virtual vertices and combining them into triangular fans. Examples include displaying droplet shapes for the precipitation data or forming line segments for the CRNS data. In addition, domain scientists have asked for the animation of cosmic ray rover data to show the route taken over the course of each day acquiring measurements. We introduced a procedurally growing line-topology mesh that is applied to the CRNS data, connecting consecutive vertex tuples to form line strips and generate a predefined number of line segments per second. Subsequently, geometry shaders are used to display the line segments with an adaptive width corresponding to the actual measurement range of the rover. In each of the above cases, the original color scheme of the point data is used to generate a texture and UV maps assigned to each vertex, so that the colour of shapes generated via transform feedback is interpolated based on the data for the original point cloud.

Different temporal scales (as shown for precipitation data and soil moisture simulation) are currently a challenge: Animations within Unity are displayed at a specified number of frames per second. This requires manual adjustment for synchronising multiple concurrent animations, which is time-consuming to configure, especially if datasets are updated or extended at certain stages of the development process. A first approach providing this functionality has been introduced to our framework for this case study, but will be refined in the future to allow for a more straightforward integration of transient datasets at different time scales.

Extensive environmental projects or initiatives require the collaboration of researchers from different scientific domains, such as geologists, physicists, hydrologists, and meteorologists. Providing an intuitive way to visualise, explore, correlate, and evaluate collections of heterogenous datasets and including numerical models to assess possible consequences of changing climate conditions provides a notable benefit to all parties involved. Typically, researchers are working with geographic information systems or other even more domain-specific software. While it is in principle possible to create animations with products such as ArcGIS or QGIS [QGI09], it is cumbersome to do so. Also, a raster animation will necessarily conceal any other data located in that same spatial frame. Displaying the results of numerical simulations is not possible at all. So visualising multiple datasets located within the same region in 3D, integrating observation and simulation data in the same geographic context, and animating (multiple) 2D/3D datasets are significant advantages of our framework for the exploration of complex environmental data collections and the evaluation of specific datasets. An obvious example for the above is the concurrent visualisation of (observed) precipitation data and (simulated) soil moisture, where the delayed regional increase of soil moisture after a rain event shows a concrete correlation of both datasets (see Figs. 1 and 6d). Spatial or temporal mismatches become obvious even at a superficial visual inspection. In addition, an (immersive) visualisation such as this is very useful for outreach activities. It illustrates the rationale of doing such complex measurements in the first place, shows intuitively how datasets correlate to form a larger picture and facilitate the understanding of complex environmental phenomena. On the other hand, our framework does not support analytic tasks that require accessing the raw data, such as reading specific data values for an arbitrary location as well as performing measurements, calculations, or applying (non-)linear filters on input data sets.

While the intended use of this geographic environment is a virtual reality environment (either a CAVE or head-mounted display), it also works on a regular stand-alone machine using a standard screen. The application is interactive, users can explore the scene via keyboard/mouse or via specific VR input devices, such as a Flystick or HTC Vive Controllers. Supplemental data can be linked to 3D datasets and accessed by picking a dataset in the scene (such as the time series data displayed in Fig. 4b). A menu allows to automatically move to points of interest, datasets can switched on or off (or have their transparency adjusted), and there is a basic media player-inspired interface for displaying animations. In addition, Unity allows scripting and recording interactive sessions, resulting in a film to be presented whenever interactive presentations are not an option.

At this point, presentations of the interactive prototype of the Müglitz catchment for a larger audience has not been possible due to COVID restrictions. However, feedback on the prototype by selected domain scientists has been very positive, in particular regarding the possibilities for outreach activities. In addition, the resulting collection of file converters, pre-processing tools, and Unity extensions allows to quickly set up new scenes for different regions of interest, without additional programming or considering technical aspects of the subsequent architecture used for presentation.

5. Conclusions

We presented a Virtual Geographic Environment for the exploration of hydro-meteorological extremes based on an extended Unity framework. Including a wide range of datasets acquired via state-of-the-art as well as experimental measurement techniques, the VGE gives a comprehensive overview of the data collected within the region of interest. In addition, results of various numerical models add area-wide information on processes on and below the surface, resulting in a broad impression on multiple environmental compartments within one unified geographic context. It allows a concurrent visualisation of multiple datasets located in the same

geographic region in a way that would be challenging or even impossible using established software such as geographic information systems. Of particular importance was the synchronised animation of multiple 2D/3D datasets with varying spatial and temporal resolution. Linking additional data such as documents, plots, or images to objects within the scene allows for the extension of the VGE into an interactive environmental information system. The resulting application can be easily extended and the application of the framework for a different regions of interest is straightforward. While performing analytic tasks that require access to the raw data are not possible using our framework, it provides insight into the interrelation of multiple datasets from different compartments and acquired via various observation techniques or numerical simulation codes.

In the scope of the MOSES initiative, there is still a large collection of datasets available not yet included in this study. An obvious addition is runoff data measured at various locations along the river network as well as simulated using the hydrological model, both of which have not yet been added to the prototype. Extending the existing groundwater model to show transient changes, especially during flood/draught events, will help to improve the understanding of phenomena related to the water cycle and the consequences for agriculture and the ecosystem in general. Regarding data visualisation, a demonstrative comparison of measured and simulated data will be a large benefit, both for researchers evaluating their data as well as for consolidating confidence in numeric modelling results in general. Given the scheduled measurement campaigns and the focus on short term meteorological and hydrological events, a more versatile global management of temporal relationships between datasets and more sophisticated functionality for displaying synchronised animations with different temporal discretisation is also a challenge that requires more attention in future developments of our framework.

Acknowledgements: This work was supported by the Helmholtz Association in the framework of MOSES (Modular Observation Solutions for Earth Systems). The Virtual Campaign development and demonstration is part of the projects "Advanced Earth System Modelling Capacity (ESM)" and "Digital Earth", both funded by the Initiative and Networking Fund of the Helmholtz Association.

References

[AGL05] AHRENS J., GEVECI B., LAW C.: ParaView: An End-User Tool for Large Data Visualization. In *The Visualization Handbook*, Hansen C., Johnson C., (Eds.). Elsevier, 2005. 3

[Bat97] BATTY M.: Virtual geography. *Futures 29* (1997), 337–352. doi:10.1016/S0016-3287(97)00018-9. 3

[Bat08] BATTY M.: Virtual reality in Geographic Information Systems. In *The Handbook of Geographic Information Science*, Wilson J., Fotheringham A., (Eds.). Blackwell Publishing, Oxford, UK, 2008, pp. 317–334. 3

[BBH*15] BAATZ R., BOGENA H. R., HENDRICKS FRANSSEN H.-J., ET AL.: An empirical vegetation correction for soil water content quantification us-ing cosmic-ray probes. *Water Resour Res 51* (2015), 2030–2046. doi:10.1002/2014WR016443. 4

[Bun21] BUNDESAMT FÜR KARTOGRAPHIE UND GEODÄSIE: GeoBasis-DE, 2021. *(downloaded via Google Earth)*. 3

[CCGG96] COOK S. E., CORNER R. J., GROVES P. R., GREALISH G. J.: Use of airborne gamma radiometric data for soil mapping. *Aust J Soil Res 34* (1996), 183–194. 5

[CSC16] CHO Y., SUDDUTH K. A., CHUNG S.-O.: Soil physical property estimation from soil strength and apparent electrical conductivity sensor data. *Biosystems Eng 152* (2016), 68–78. doi:10.1016/j.biosystemseng.2016.07.003. 5

[Des17] DESILETS D.: Overview of the cosmic ray technique including measurement principles and calculation. In *Cosmic Ray Neutron Sensing: Use, Calibration, and Validation for Soil Moisture Estimation*. International Atomic Energy Agency, 2017. IAEA-TECDOC-1809, ISBN:978-92-0-101017-9. 4

[Deu19] DEUTSCHER WETTERDIENST: RADOLAN (Radar-Online-Aneichung). https://www.dwd.de/DE/leistungen/radolan/radolan.html, 2019. 3

[DW13] DIERKE C., WERBAN U.: Relationships between gamma-ray data and soil properties at an agricultural test site. *Geoderma 199* (2013), 90–98. doi:10.1016/j.geoderma.2012.10.017. 5

[Ell94] ELLIS S. R.: What are virtual environments? *IEEE Comput Graph Appl 14* (1994), 17–22. doi:10.1109/38.250914. 3

[GFW17] GU S., FANG C., WANG Y.: Virtual geographic environment for WATLAC hydrological model integration. In *Proc of 25th International Conference on Geoinformatics* (2017), IEEE Computer Society. doi:10.1109/GEOINFORMATICS.2017.8090931. 2

[KBB*12] KOLDITZ O., BAUER S., BILKE L., ET AL.: OpenGeoSys: An open source initiative for numerical simulation of thermo-hydro-mechanical/chemical (THM/C) processes in porous media. *Environ Earth Sci 67*, 2 (2012), 589–599. doi:10.1007/s12665-012-1546-x. 5

[KHS*18] KERN M., HEWSON T., SCHÄFLER, ET AL.: Interactive 3D Visual Analysis of Atmospheric Fronts. *IEEE Trans Visual Comput Graph 25* (2018), 1080–1090. doi:10.1109/TVCG.2018.2864806. 3

[KSA13] KUMAR R., SAMANIEGO L., ATTINGER S.: Implications of distributed hydrologic model parameterization on water fluxes at multiple scales and locations. *Water Resour Res 49*, 1 (2013). doi:10.1029/2012WR012195. 5

[KvdN18] KOUTEK M., VAN DER NEUT I.: Web-based 3D Meteo Visualization: 3D Rendering Farms from a New Perspective. In *Proc of Workshop on Visualisation in Environmental Sciences (EnvirVis)* (2018), The Eurographics Association. doi:10.2312/envirvis.20181132. 3

[LCL*13] LIN H., CHEN M., LU G., ET AL.: Virtual Geographic Environments (VGEs): A New Generation of Geographic Analysis Tool. *Earth Sci Rev 126* (2013), 74–84. doi:10.1016/j.earscirev.2013.08.001. 2, 3

[LYZ*15] LÜ G., YU Z., ZHOU L., ET AL.: Data environment construction for virtual geographic environment. *Environ Earth Sci 74* (2015), 7003–7013. doi:10.1007/s12665-015-4736-5. 2

[MWZ*17] MARTINI E., WERBAN U., ZACHARIAS S., ET AL.: Repeated electromagnetic induction measurements for mapping soil moisture at the field scale: Validation with data from a wireless soil moisture monitoring network. *Hydrol Earth Syst Sci 21* (2017), 495–513. doi:10.5194/hess-21-495-2017. 5

[QGI09] QGIS DEVELOPMENT TEAM: QGIS Geographic Information System. http://qgis.osgeo.org, 2009. 7

[RBK14] RINK K., BILKE L., KOLDITZ O.: Visualisation Strategies for Environmental Modelling Data. *Environ Earth Sci 72*, 10 (2014), 3857–3868. doi:10.1007/s12665-013-2970-2. 3, 5

[RCB*18] RINK K., CHEN C., BILKE L., LIAO Z., RINKE K., FRASSL M., YUE T., KOLDITZ O.: Virtual geographic environments for water pollution control. *Int J Dig Earth 11*, 4 (2018), 397–407. doi:10.1080/17538947.2016.1265016. 3

[RNZ*20] RINK K., NIXDORF E., ZHOU C., HILLMANN M., BILKE L.: A Virtual Geographic Environment for Multi-Compartment Water and Solute Dynamics in Large Catchments. *J Hydrol 582* (2020), art. 124507. doi:10.1016/j.jhydrol.2019.124507. 2, 3, 6

[RWA*20] RENTSCHLER T., WERBAN U., AHNER M., ET AL.: 3D mapping of soil organic carbon content and soil moisture with multiple geophysical sensors and machine learning. *Vadose Zone Journal 19*, e20062 (2020). doi:10.1002/vzj2.20062. 5

[Sae20] SAECHSISCHES STAATSMINISTERIUM FÜR ENERGIE, KLIMASCHUTZ, UMWELT UND LANDWIRTSCHAFT: Bodenkarte 1 : 50.000 (BK50). https://www.boden.sachsen.de/digitale-bodenkarte-1-50-000-19474.html, 2020. Metadaten-ID:b826fa66-e20d-40b2-868b-234cbe5333dc. 5

[SHB*14] SCHWARZE R., HAUFFE C., BALDY A., ET AL.: *Klimawandel und Wasserhaushalt in Sachsen*, vol. 32/2014 of *Schriftenreihe des LfULG*. Sächsisches Landesamt für Umwelt, Landwirtschaft und Geologie, 2014. ISSN:1867-2868. 3, 5, 7

[SKA10] SAMANIEGO L., KUMAR R., ATTINGER S.: Multiscale parameter regionalization of a grid-based hydrologic model at the mesoscale. *Water Resour Res 46*, 5 (2010). doi:10.1029/2008WR007327. 5

[SML06] SCHROEDER W., MARTIN K., LORENSEN B.: *Visualization Toolkit: An Object-Oriented Approach to 3D Graphics (4th Edition)*. Kitware, Inc., 2006. 3

[SRK*18] SCHRÖN M., ROSOLEM R., KÖHLI, ET AL.: Cosmic-ray neutron rover surveys of field soil moisture and the influence of roads. *Water Resour Res 54* (2018), 6441–6459. doi:10.1029/2017WR021719. 4

[Sta15] STAATSBETRIEB GEOBASISINFORMATION UND VERMESSUNG SACHSEN: Digitales Geländemodell 2. https://www.geodaten.sachsen.de/digitale-hoehenmodelle-3994.html, 2015. Metadaten-ID:a3dba5b2-0118-4d76-ab78-ba656a1b489e. 3

[Uni18] UNITED STATES GEOLOGICAL SURVEY: Shuttle Radar Topography Mission 1 Arc-Second Global, 2018. doi:10.5066/F7PR7TFT. 3

[Uni20] UNITY TECHNOLOGIES: Unity (Version 2020.1). https://unity3d.com/, 2020. 3

[Yin10] YIN L.: Integrating 3D Visualization and GIS in Planning Education. *J Geogr High Educ 34*, 3 (2010), 419–438. 3